IEEE Access
Multidisciplinary ⋮ Rapid Review ⋮ Open Access Journal

Received 17 March 2023, accepted 20 April 2023, date of publication 1 May 2023, date of current version 10 May 2023.

Digital Object Identifier 10.1109/ACCESS.2023.3271969

RESEARCH ARTICLE

Design Optimization of Noise Filter Using Quantum Annealer

AKIHISA OKADA[1], HIROAKI YOSHIDA[1], KIYOSUMI KIDONO[1], TADAYOSHI MATSUMORI[2], TAKANORI TAKENO[2], AND TADASHI KADOWAKI[2]

[1]Toyota Central Research and Development Labs Inc., Tokyo 112-0004, Japan
[2]Denso Corporation, Tokyo 108-0075, Japan

Corresponding author: Akihisa Okada (a-okada@mosk.tytlabs.co.jp)

ABSTRACT The use of quantum annealers in black-box optimization to obtain the desired properties of a product with a small number of trials has attracted attention. However, the application of this technique to engineering design problems has been limited. Here, we demonstrate the applicability of black-box optimization with a quantum annealer to the design of electric circuit systems, focusing on π-type noise filters as an example. We develop a framework that uses quantum annealing to find the optimal location of electrical components and conductor paths connecting the components, and confirm that the learning process appropriately works over a number of trials to efficiently search for a design with high performance. The results show the potential applicability of quantum annealing to design problems of electric circuit systems.

INDEX TERMS Combinatorial optimization problem, noise filter, quadratic unconstrained binary optimization, quantum annealing, quantum computing.

I. INTRODUCTION

A. QUANTUM ANNEALERS

High-performance computers are required to elucidate and predict complex phenomena, such as in simulations of the behavior of systems with multiple interconnected factors. However, Neumann-type computers, whose development has followed Moore's law, do not meet the demand for high performance. Drastic improvements in Neumann-type computers are not expected [1] as their single-threaded performance has reached its ceiling [2]. Therefore, non-Neumann-type computers are expected to be an alternative for high-performance computation for complex problems.

Quantum annealers are one type of non-Neumann-type computer [3]. Commercial machines are available from D-Wave Systems. The architecture of a quantum annealer implements the Ising model on a circuit using superconductivity. The ground state of the Ising model is efficiently found using the quantum effect [4], [5], [6].

Since the ground state of the Ising model is equivalent to the solution of quadratic unconstrained binary optimization (QUBO), which includes not only fundamental problems [7] but also practical ones [8], [9], [10], [11], [12], [13], [14], a quantum annealer is regarded as a quantum solver for QUBO problems.

Pragmatically, the usability of quantum annealers for complex problems relies on their compatibility with the QUBO formulation. Previous studies are limited to cases in which the original problem formulation has an apparent link to QUBO, such as that for combinatorial optimization problems. A recent study combined quantum annealing with machine learning to find the optimal arrangement of the constituent elements of a metamaterial [15]. The original problem (optical properties of the metamaterial) was not necessarily converted to a QUBO formulation, implying the applicability of quantum annealing to general optimization problems. Specifically, they proposed a type of black-box optimization framework, in which the unknown relation between the input binary variables and the complex property values computed according to the governing equations is learned by means of a second-order regression equation and the optimal input variables are obtained using quantum annealing.

Reports of applying black-box optimization to design problems are limited to optical problems with the optimal arrangement of metamaterials described above and

The associate editor coordinating the review of this manuscript and approving it for publication was Wei Huang.

photonic-crystals [16], the structural dynamics problem of substrate vibration [17], and molecular design [18].

B. DESIGN PROBLEM OF NOISE FILTER

In this study, we focus on an electric noise filter as an example electric circuit. Noise filter performance depends on the combination of electrical components and the paths of conductors connecting them.

Products designed for electromagnetic compatibility incorporate noise filters that reduce input voltage noise to prevent high-frequency noise from affecting surrounding electronic devices, which are low-pass filters. The electrical component allocation region needs to be determined under the constraint of a certain amount of noise attenuation, i.e., an optimal filter design is required. In this study, we apply black-box optimization that incorporates calculations conducted using quantum annealing to the design optimization of a noise filter that consists of two capacitors and an inductor, called a π-type filter, and demonstrate that this optimization framework is useful for electric circuit design problems.

Topology optimization has been used for optimal design. Although topology optimization is applicable to electric circuits [19], the inherent challenge is to avoid falling into a local optimal solution, which stems from the method being based on the gradient method. In particular, optimization problems with many degrees of freedom related to element location, as considered in this study, generally have a complex objective function space, which can hinder the search for the global optimal solution. The proposed optimization framework, which combines black-box optimization and quantum annealing, exploits the features of quantum annealing to avoid becoming trapped in a local optimal solution.

C. SUMMARY OF CONTRIBUTIONS

The contributions of this study can be summarized as follows.

- We extend the framework of optimal design based on black-box optimization using quantum annealing to problems related to electric circuit systems.
- We confirm that the optimization process works as an optimal design method for electric circuits by analyzing the learning process based on the relation between the number of searches and performance values.

II. METHOD

A. DESIGN PROBLEM OF π-TYPE NOISE FILTER

A circuit diagram of the π-type noise filter to be designed is shown in Fig. 1. The circuit consists of three elements, namely an inductor and two capacitors. Figure 2 shows the π-type noise filter model utilized in this study. It is assumed that the back side of the substrate is grounded. The performance of a noise filter is determined by the capacitance of the capacitor, the inductance of the inductor, inductive noise, and parasitic capacitance. The inductive noise and parasitic capacitance depend on the relative location of the inductor, the capacitors, and the conductor path, which does not appear in the circuit diagram but should be designed as described below.

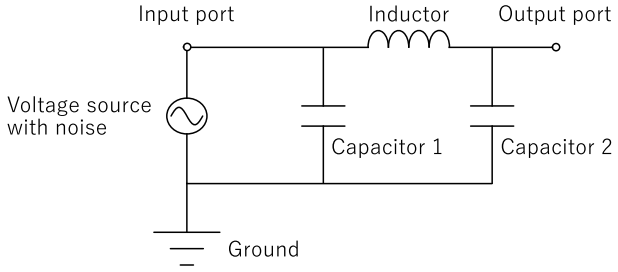

FIGURE 1. Circuit diagram of π-type noise filter.

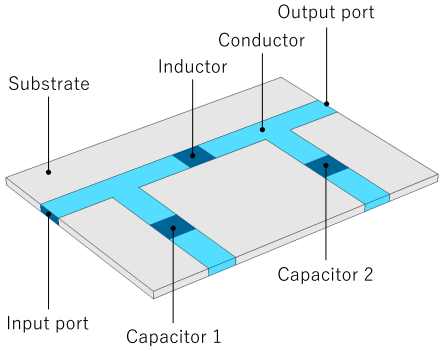

FIGURE 2. Example of element and conductor arrangement for π-type noise filter. The input and output ports, capacitors, and inductor are represented by simple square elements. The backplane is the electrical ground.

B. BLACK-BOX OPTIMIZATION OF NOISE FILTER

The objective of black-box optimization is to obtain the input parameter x that minimizes (or maximizes) the characteristic value y with a small number of trials under the condition that the relation between x and y ($y = f(x)$) is unknown. Here, we focus on Bayesian Optimization of Combinatorial Structures (BOCS) [20], which is a learning method applicable to cases where the input parameter x is a binary variable, as done in the literature [21]. In BOCS, the relation between x and y is learned sequentially using a quadratic regression equation of x. In other words, starting with several data sets of x and y, we (1) obtain the data y for the input x through simulations or experiments on a real system where the input-output relation is unknown, (2) learn the relation between data y and input x in quadratic form, and (3) search for the optimal input x under the assumed quadratic relation. The relation between the various tasks in BOCS is summarized in Fig. 3.

To apply this black-box optimization to the design of noise filters, we define a binary variable x that specifies the location of the element and the conductor path, and employ electromagnetic field analysis using the finite element method as the data acquisition method in (1). In (3), quantum annealing is employed to find the global minimum in the regression model, which has many local minima. The solution x of the quantum annealing and the corresponding output value y

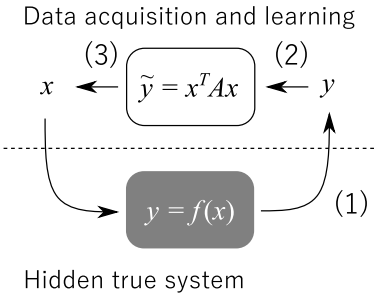

FIGURE 3. Schematic diagram of BOCS. (1) Data y for input x is obtained from simulation or experiment. (2) Second-order regression equation is estimated from input x and y. $\tilde{y}$ is estimated value. (3) Optimal x is found. Here, A is the coefficient of the quadratic regression equation. f is an unknown function under the governing equation.

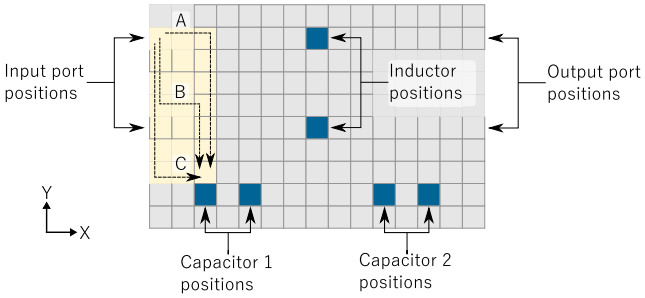

FIGURE 4. Candidate element positions and conductor paths. As an example of conductor paths, three candidates (A, B, and C) between the upper side of the input port and the left side of capacitor 1 are shown.

are added to the data in the learning process. We refer to this method as BOCS-QA. To clarify the effect of quantum annealing, a calculation using simulated annealing (BOCS-SA) instead of quantum annealing is also performed and the results are compared. Explanations for the quantum annealing and simulated annealing are given in Sec. II-C below.

The following sections describe the binary design variables that represent electrical component positions and conductor paths and the characteristic values for evaluating filter performance.

1) BINARY DESIGN VARIABLES

The element positions and conductor paths between the elements are mapped to the binary variable x. In this study, the problem is to select the positions of five elements (an input port, an output port, an inductor, and two capacitors) from two candidates and the conductor paths from three candidates. In order to represent these variables as binary variables, the substrate is divided into a 10×15 (X×Y) grid. The input and output ports are placed on the sides of the board and the inductor and capacitor are placed in the grid as concentrated elements, as shown in Fig. 4.

Three candidate paths as conductors are created by connecting the elements from top to bottom in the following manner.

A. Draw a path in the X direction and then in the Y direction.

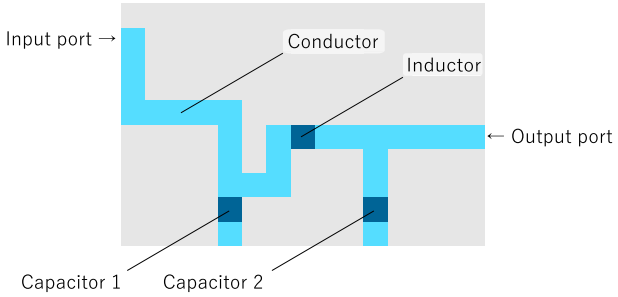

FIGURE 5. Circuit corresponding to bit string "01011010100100011100100" in one-hot representation.

B. Draw a path in the Y direction to half of the difference, then in X, and then in the remaining Y direction.

C. Draw a path in the Y direction and then in the X direction.

The typical π-type noise filter, shown in Fig. 2, is appropriately included as a candidate by the above conductor setting. The present method can be simply extended to the case with more than three candidate paths if necessary.

We adopt one-hot encoding to represent noise filters in which element positions and conductor paths are selected from these candidates. In the case considered here, 22 bits are required because there are two candidates for each of the five element positions and three candidates for each of the four conductor paths. Let "10" be the state in which the element is at the bottom or on the left and "01" be the state in which it is at the top or on the right. Then, let "100" be a conductor path that first moves in the X direction, "010" be one that turns in the middle, and "001" be one that first moves in the Y direction. The bits that represent the conductor path follow the element position bits; that is, the first 10 bits represent the five element positions and the latter 12 bits represent the selection of the four conductor paths. The bits that represent the element positions are arranged on the board in the following order from left to right: input port, capacitor 1, inductor, capacitor 2, and output port. The conductor paths are similarly arranged in the following order from left to right: input port - capacitor 1, capacitor 1 - inductor, inductor - capacitor 2, and capacitor 2 - output port. For example, a circuit encoded by "01011010100100011100100" as binary variable x is shown in Fig. 5. Note that we adopted one-hot encoding for qubit encoding in order to allow multiple selections for conductor paths and exclusive selections for element positions, which is not implemented directly using domain-wall or binary encoding.

2) OBTAINING CHARACTERISTIC VALUE

The S-parameter S_{21} is adopted as the characteristic value y of the noise filter. S_{21} indicates the ratio of output power to input power. When the input power of noise is p_1 and the output power is p_2, S_{21} is expressed by the following equation,

$$S_{21} = \sqrt{\frac{|p_2|}{|p_1|}}. \tag{1}$$

We design a noise filter that minimizes S_{21} under the given noise voltage. p_1 and p_2 are calculated using finite element analysis for simulating the electromagnetic field of the electric circuit model shown in Fig. 2. The governing equations utilized in the finite element method are Maxwell's equations in the frequency domain with a constitutive equation for the materials as follows:

$$\nabla \times (\nabla \times \boldsymbol{E}) - \varepsilon\mu\omega^2 \left(1 - \frac{j\sigma}{\omega\varepsilon}\right) \boldsymbol{E} = \boldsymbol{0}, \tag{2}$$

where $\boldsymbol{E}$, μ, ε, σ, ω, j is the electric field, permeability, permittivity, electrical conductivity, electric field frequency, imaginary unit, respectively. With this equation, the currents induced by high-frequency input voltages are taken into account.

In the electric circuit model, the back of the board is the ground and the electrical components are lumped-parameter ones on the surface of the board. A sufficiently large air region is provided around the board in order to precisely calculate the induced noise. A scattering boundary condition is set at the outermost boundary of the air region.

Special procedures are required in the following two cases where the S-parameters are not correctly evaluated by the finite element method.

(I) Element position does not satisfy the one-hot constraint.
(II) A bit in the conductor path is "000" (the circuit has a disconnection on the board).

In case (I), the binary variables are unencodable to a configuration of a noise filter. Given such binary variables, instead of performing the finite element method, we calculate y as a penalty according to the following formula,

$$y = y_{\text{base}} + \lambda \sum_{m=1}^{5} (x_{2m-1} + x_{2m} - 1)^2, \tag{3}$$

where y_{base} is the base value of the violation of one-hot constraints, λ is the penalty coefficient, and x_i is the value of the i-th bit of the binary variable x. Since BOCS learns characteristic values in quadratic form, this penalty of one-hot constraints is also expected to be learned.

In case (II), meaningful S-parameters for evaluating a noise filter performance cannot be obtained because the conductor path is disconnected such that voltage is conducted neither from a normal signal nor noise. We assign a dummy conductor that avoids the disconnection, as shown in Fig. 6. Note that when multiple conductor paths are selected, such as "011", we take the sum of the conductor paths.

To summarize, we calculate the characteristic value of a noise filter y using the following equation,

$$z \equiv \sum_{m=1}^{5} (x_{2m-1} + x_{2m} - 1)^2, \tag{4}$$

$$y = \begin{cases} S_{21} & (\text{ for } z = 0\ ), \\ y_{\text{base}} + \lambda z & (\text{ for } z \neq 0\ ). \end{cases} \tag{5}$$

FIGURE 6. Circuit corresponding to bit string "100101100100000100010 0". The conductor paths between the input power port and capacitor 1 and those between the inductor and capacitor 2 are not selected. To avoid disconnection, conductors spread over the board are assigned.

C. NUMERICAL EXPERIMENT

1) CHARACTERISTIC VALUES

To conduct the electromagnetic field simulation on the basis of a finite element method, we employed the COMSOL Multiphysics software [22]. As a circuit model for finite element method, the substrate thickness, width, and height are set to 1.6, 150, and 100 mm, respectively. An air area of 30 mm is provided around the board. Scattering boundary conditions are set at the outermost boundaries of this air region. The substrate is divided into a 10×15 grid, as introduced in section II-B1.

The physical constants of the power supply port, capacitor, and inductor are set to 50 Ω, 100 F, and 10 H, respectively. The substrate's relative permittivity, relative permeability, and conductivity are set to 4.5, 1, and 1.0×10^{-8} S/m, respectively, assuming an FR-4 substrate. The conductor is treated as a perfect conductor. In addition, S_{21} was calculated using a frequency analysis at 10 MHz.

For Eq. (3), we set $y_{\text{base}} = -60$ and $\lambda = 10$. This λ was calibrated to such an extent that any violation causes a deterioration in the characteristic value S_{21}, thereby compelling a quest for a π-type noise filter. If the value of λ is small (~ 1), we have confirmed that we need a greater number of searches to find a solution that satisfies the constraints in an auxiliary calculation. We avoided using too large a value of lambda because the accuracy of learning the optimal value in the absence of element violations would suffer.

2) QUANTUM ANNEALING

The quantum approach for optimizing binary variables is realized with the following Hamiltonian system [4]:

$$\mathcal{H} = -(1-\alpha) \sum_i \sigma_x^{(i)} + \alpha \left(\sum_i h_i \sigma_z^{(i)} + \sum_{i>j} J_{i,j} \sigma_z^{(i)} \sigma_z^{(j)} \right), \tag{6}$$

where superscript i is an index of spin location. σ_x, σ_z are x and z component of Pauli matrices operating on spins. h_i is external magnetic field and $J_{i,j}$ is coupling strength between spin i and spin j. The second term on right-hand side is the target Ising model, which is equivalent to the QUBO formula by variable conversion $x = (1 - \sigma_z)/2$. When we

adiabatically increase α from 0 to 1, we obtain the ground state of the Ising model, i.e., the resulting spins σ_x correspond to the binary values optimized for the problem specified by h_i and $J_{i,j}$.

The quantum annealer practically used was Advantage_system4.1 provided by D-Wave Systems. We utilized default setting of the time schedule of α in Eq. 6. The sampling number was set to 3000 when solving the problem. The x value that gave the smallest y was adopted as the next candidate.

3) SIMULATED ANNEALING

One of the classical counterparts of quantum annealing is simulated annealing, which is a stochastic optimization algorithm. This method is also capable of searching the ground state of the Ising model. It starts with an initial configuration of spins and randomly selects spin to flip. Then, the algorithm decides whether to accept or reject the new configuration based on the acceptance probability which is calculated using the Metropolis-Hastings algorithm: $P = \exp(-\Delta E/T)$, where P is the acceptance probability, ΔE is the difference in energy between the new and current configuration, and T is the current temperature of the system. The temperature is gradually reduced over time to escape local optima and explore the solution space effectively.

We adopted the Python library "dwave-neal" by D-Wave Systems [23] as a simulated annealing method. The default settings of this library for the parameters of simulated annealing were used, in which the initial state was randomly selected and the cooling schedule was geometric. The sampling number was set to 3000, and x that gave the smallest y was selected as the next candidate, which was the same as quantum annealing.

4) BOCS SETTING

For the initial training datasets of BOCS, we prepared 20 randomly generated binary variables x and their corresponding characteristic values y. BOCS-QA and -SA were performed until 300 searches were conducted.

III. RESULTS AND DISCUSSION

We compare the results of the BOCS-QA and BOCS-SA calculations with those of random search in which binary variables were randomly generated.

First, the results of all search histories of BOCS-QA and random search are shown in Figs. 7 and 8, respectively.

The learning processes of BOCS-QA and random search are different. Figure 7 shows that BOCS-QA mainly learned the penalty term in Eq. (3) in the beginning (before approximately 60th search), and subsequently started to learn on the bases of the performance of the noise filter S_{21}, suggesting that the design of the penalty term facilitated learning. Then, the highest record of S_{21} was steadily set. On the other hand, the random search shown in Fig. 8 searched for a feasible noise filter in very rare cases. There is no particular trend. The number of solutions that satisfy the one-hot constraint is ten, which is close to the expected value. The probability that a random binary variable satisfies the one-hot constraint is $2^5/2^{10} = 1/32$, so the expected number for 300 searches is nine.

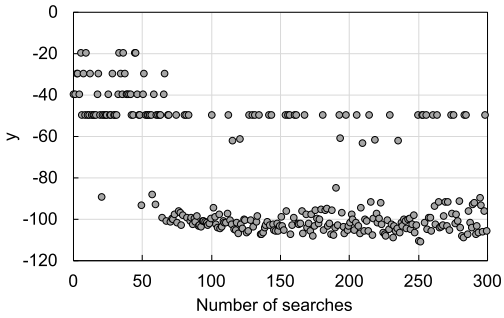

FIGURE 7. Full search history of BOCS-QA.

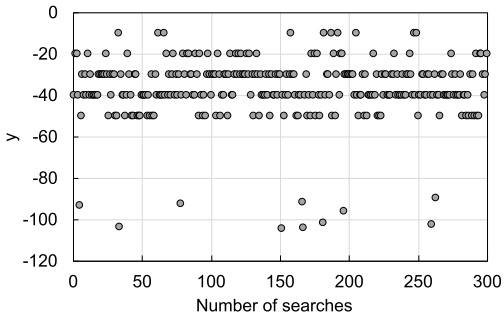

FIGURE 8. Full search history of random search.

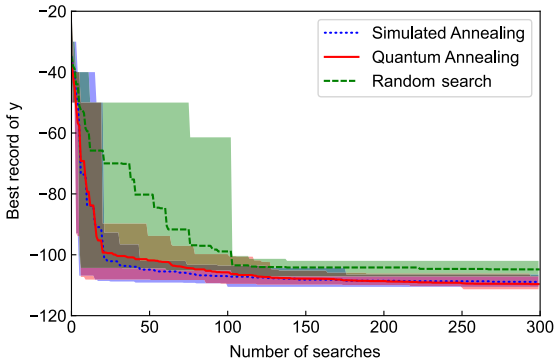

FIGURE 9. Updated records of y. The solid and dotted lines represent the mean and the filled area represents the area between the maximum and minimum values.

The update records of the characteristic value y versus the number of searches are shown in Fig. 9. Since BOCS-QA, BOCS-SA, and random search are randomized algorithms, the mean, minimum, and maximum values were calculated for ten trials. BOCS-QA and BOCS-SA steadily search for a noise filter with good performance, whereas random search tends to have a large variance (especially with a small number of searches). The steady performance improvement of BOCS-QA and BOCS-SA shown in Fig. 9 is due to the successful learning of S_{21}, as confirmed in Fig. 7. At 300 searches, BOCS-QA shows slightly better

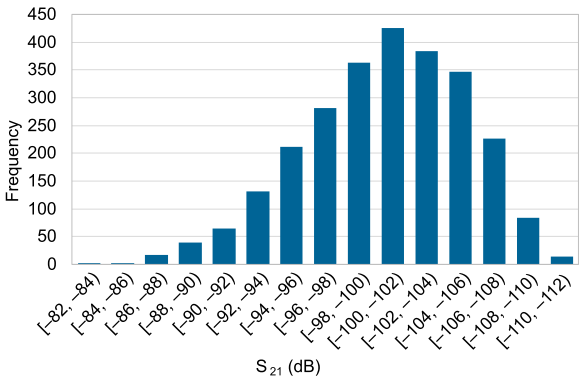

FIGURE 10. Histogram of S_{21} value in decibels when element positions are specified uniquely and there is one conductor between elements.

TABLE 1. Comparison of results obtained by various methods.

Method	Object	Value	Rank
QA	Best	−111.34 dB	1st
	Average	−109.64 dB	19th
	Worst	−106.97 dB	192nd
SA	Best	−110.55 dB	14th
	Average	−108.91 dB	48th
	Worst	−104.80 dB	528th
Random	Best	−107.12 dB	180th
	Average	−104.80 dB	192th
	Worst	−102.00 dB	1058th

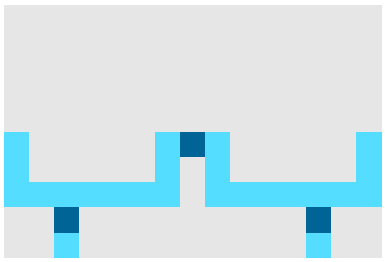

FIGURE 11. Noise filter obtained by BOCS-QA.

performance than that of BOCS-SA in terms of the average, minimum, and maximum values, as shown in Table 1.

Next, we evaluate the filter performance of the obtained solution. Since there are 2^{22} cases (expressed in 22 bits), enumerating the performance of all solutions is unrealistic. We therefore choose only the relevant solutions with unique element positions and a single conductor path between elements. This gives a total of 2592 cases ($2^5 = 32$ combinations of element positions and $3^4 = 81$ combinations of conductor positions). Figure 10 shows a histogram of the S_{21} value in decibels. For our settings, noise filters whose S_{21} is under −108dB are rare (approximately 3%). Since the average records of BOCS-QA and BOCS-SA are in the top 0.8% and 1.9%, respectively, as shown in Tabl. 1, these methods finding such filters in 300 searches are considered efficient.

The configuration of the best-performing noise filter obtained using BOCS-QA is shown in Fig. 11. In this case, the value of S_{21} was −111.34 dB. The input port and capacitor are placed close to each other, preventing performance degradation due to induced noise. This shows that the obtained configuration is physically reasonable.

In this study, we formulated a problem with two candidates for the element positions and three candidates for the conductor paths. If we considered a large-scale problem with a larger number of candidates, the probability of finding a well-posed noise filter by chance using random search would be much smaller and the superiority of BOCS-QA and BOCS-SA would be more significant.

IV. CONCLUSION AND OUTLOOK

To find input parameters that provide the desired characteristics with a small number of searches, we proposed an iterative optimization method that incorporates quantum annealing in the BOCS framework and applied it to the problem of designing noise filters. A π-type noise filter that consists of two capacitors and an inductor was considered. A model was created to select two candidates for the location of these elements and three candidates for the path of the conductor connecting the elements. The results show that a high-performance noise filter can be efficiently found and that the search progresses more stably than does random search. This shows that the framework that incorporates quantum annealing into black-box optimization is applicable to electric circuit design problems. The present method could help engineers meet the high demand for electrical products.

Beyond the optimization of electric components demonstrated here, system-level optimization of electric devices is a topic for future work. It could lead to multiphysics optimal design that requires simultaneous optimizations of multiple phenomena.

The proposed BOCS framework was proven to work with quantum annealing and simulated annealing. A comparison of these two versions showed only a slight difference. A recent study that compared the two solvers in a black-box optimization framework also concluded that clear performance improvements using quantum annealing are rare [17]. However, a clear advantage of quantum annealing in finding optimal solutions, achieved by adjusting the annealing schedule, has recently been reported [24]. Future research should thus examine in detail the scheduling protocols to further improve the performance of BOCS with quantum annealing. In addition, a recent improvement of the learning process [21] could be integrated into the present BOCS framework to speed up the whole optimization process.

REFERENCES

[1] G. E. Moore, "Cramming more components onto integrated circuits, reprinted from electronics," *IEEE Solid-State Circuits Soc. Newslett.*, vol. 11, no. 3, pp. 33–35, Sep. 2006, doi: 10.1109/N-SSC.2006.4785860.
[2] C. Moore, "Data processing in exascale-class computer systems," in *Proc. Salishan Conf. High Speed Comput.*, 2011, pp. 1–10.
[3] M. W. Johnson et al., "Quantum annealing with manufactured spins," *Nature*, vol. 473, no. 7346, pp. 194–198, 2011, doi: 10.1038/nature10012.
[4] T. Kadowaki and H. Nishimori, "Quantum annealing in the transverse Ising model," *Phys. Rev. E, Stat. Phys. Plasmas Fluids Relat. Interdiscip. Top.*, vol. 58, no. 5, pp. 5355–5363, Nov. 1998, doi: 10.1103/PhysRevE.58.5355.

[5] E. Farhi, J. Goldstone, S. Gutmann, J. Lapan, A. Lundgren, and D. Preda, "A quantum adiabatic evolution algorithm applied to random instances of an NP-complete problem," *Science*, vol. 292, no. 5516, pp. 472–475, 2001, doi: 10.1126/science.1057726.

[6] T. Albash and D. A. Lidar, "Adiabatic quantum computation," *Rev. Mod. Phys.*, vol. 90, Jan. 2018, Art. no. 015002, doi: 10.1103/RevModPhys.90.015002.

[7] A. Lucas, "Ising formulations of many NP problems," *Frontiers Phys.*, vol. 2, pp. 1–10, Jan. 2014, doi: 10.3389/fphy.2014.00005.

[8] M. Ohzeki, A. Miki, M. J. Miyama, and M. Terabe, "Control of automated guided vehicles without collision by quantum annealer and digital devices," *Frontiers Comput. Sci.*, vol. 1, pp. 1–10, Nov. 2019, doi: 10.3389/fcomp.2019.00009.

[9] N. Nishimura, K. Tanahashi, K. Suganuma, M. J. Miyama, and M. Ohzeki, "Item listing optimization for E-commerce websites based on diversity," *Frontiers Comput. Sci.*, vol. 1, p. 2, Jul. 2019. [Online]. Available: https://www.frontiersin.org/article/10.3389/fcomp.2019.00002

[10] Z. I. Tabi, A. Marosits, Z. Kallus, P. Vaderna, I. Godor, and Z. Zimboras, "Evaluation of quantum annealer performance via the massive MIMO problem," *IEEE Access*, vol. 9, pp. 131658–131671, 2021, doi: 10.1109/ACCESS.2021.3114543.

[11] S. Yarkoni, A. Alekseyenko, M. Streif, D. Von Dollen, F. Neukart, and T. Bäck, "Multi-car paint shop optimization with quantum annealing," 2021, *arXiv:2109.07876*.

[12] D. Inoue, A. Okada, T. Matsumori, K. Aihara, and H. Yoshida, "Traffic signal optimization on a square lattice with quantum annealing," *Sci. Rep.*, vol. 11, no. 1, p. 3303, Feb. 2021, doi: 10.1038/s41598-021-82740-0.

[13] K. Terada, D. Oku, S. Kanamaru, S. Tanaka, M. Hayashi, M. Yamaoka, M. Yanagisawa, and N. Togawa, "An Ising model mapping to solve rectangle packing problem," in *Proc. Int. Symp. VLSI Design, Autom. Test (VLSI-DAT)*, Apr. 2018, pp. 1–4, doi: 10.1109/VLSI-DAT.2018.8373233.

[14] S. Yarkoni, E. Raponi, T. Bäck, and S. Schmitt, "Quantum annealing for industry applications: Introduction and review," *Rep. Prog. Phys.*, vol. 85, no. 10, Oct. 2022, Art. no. 104001, doi: 10.1088/1361-6633/ac8c54.

[15] K. Kitai, J. Guo, S. Ju, S. Tanaka, K. Tsuda, J. Shiomi, and R. Tamura, "Designing metamaterials with quantum annealing and factorization machines," *Phys. Rev. Res.*, vol. 2, no. 1, Mar. 2020, Art. no. 013319, doi: 10.1103/PhysRevResearch.2.013319.

[16] T. Inoue, Y. Seki, S. Tanaka, N. Togawa, K. Ishizaki, and S. Noda, "Towards optimization of photonic-crystal surface-emitting lasers via quantum annealing," *Opt. Exp.*, vol. 30, no. 24, pp. 43503–43512, 2022. [Online]. Available: https://opg.optica.org/oe/abstract.cfm?URI=oe-30-24-43503

[17] T. Matsumori, M. Taki, and T. Kadowaki, "Application of QUBO solver using black-box optimization to structural design for resonance avoidance," *Sci. Rep.*, vol. 12, no. 1, p. 12143, Jul. 2022, doi: 10.1038/s41598-022-16149-8.

[18] Q. Gao, G. O. Jones, M. Sugawara, T. Kobayashi, H. Yamashita, H. Kawaguchi, S. Tanaka, and N. Yamamoto, "Quantum-classical computational molecular design of deuterated high-efficiency OLED emitters," 2021, *arXiv:2110.14836*.

[19] K. Nomura, S. Yamasaki, K. Yaji, H. Bo, A. Takahashi, T. Kojima, and K. Fujita, "Topology optimization of conductors in electrical circuit," *Struct. Multidisciplinary Optim.*, vol. 59, no. 6, pp. 2205–2225, Jun. 2019, doi: 10.1007/s00158-018-02187-2.

[20] R. Baptista and M. Poloczek, "Bayesian optimization of combinatorial structures," in *Proc. 35th Int. Conf. Mach. Learn.*, in Proceedings of Machine Learning Research, vol. 80, J. Dy and A. Krause, Eds., Jul. 2018, pp. 462–471. [Online]. Available: https://proceedings.mlr.press/v80/baptista18a.html

[21] T. Kadowaki and M. Ambai, "Lossy compression of matrices by black box optimisation of mixed integer nonlinear programming," *Sci. Rep.*, vol. 12, no. 1, p. 15482, Sep. 2022, doi: 10.1038/s41598-022-19763-8.

[22] (2020). *COMSOL Multiphysics V. 5.6*. Accessed: Apr. 26, 2023. [Online]. Available: https://www.comsol.jp/release/5.6

[23] D-Wave Systems Inc. (2021). *Dwave-Neal 0.5.9*. Accessed: Apr. 26, 2023. [Online]. Available: https://github.com/dwavesystems/dwave-neal

[24] Y. W. Koh and H. Nishimori, "Quantum and classical annealing in a continuous space with multiple local minima," *Phys. Rev. A, Gen. Phys.*, vol. 105, no. 6, Jun. 2022, Art. no. 062435, doi: 10.1103/PhysRevA.105.062435.

AKIHISA OKADA received the B.Sc. degree from Shizuoka University, in 2006, and the M.Eng. and Dr.Sc. degrees from Osaka University, in 2008 and 2011, respectively. He is currently a Researcher with Toyota Central Research and Development Labs Inc. His research interests include strongly correlated electron systems, statistical mechanics, and combinatorial optimization problems. He is a member of the Physical Society of Japan.

HIROAKI YOSHIDA received the B.Eng., M.Eng., and Dr.Eng. degrees from Kyoto University, in 2003, 2005, and 2007, respectively. He joined Toyota Central Research and Development Labs Inc., in 2007, and a leading Researcher of applied mathematics research domain. From 2015 to 2017, he was a Visiting Researcher with École Normale Supérieure, Paris. His research interests include computational physics and micro-and nano-fluidics.

KIYOSUMI KIDONO received the B.E. and M.E. degrees from Osaka University, in 1998 and 2000, respectively, and the Ph.D. degree from the Toyohashi University of Technology, in 2012. He joined Toyota Central Research and Development Labs Inc., in 2000, where he is currently an Office Manager with the Research Planning Section. From 2016 to 2017, he was with Toyota Research Institute Inc., USA. His research interests include computer vision, intelligent vehicles, and robotics.

TADAYOSHI MATSUMORI received the B.Eng., M.Eng., and Dr.Eng. degrees from Kanazawa University, in 2003, 2005, and 2008, respectively. He joined Toyota Central Research and Development Labs Inc., in 2009. Since 2020, he has been with Denso Corporation. His research interests include optimum structural design and computational engineering.

TAKANORI TAKENO received the B.Eng., M.Eng., and Ph.D. degrees from Tohoku University, in 2003, 2005, and 2007, respectively. He was an Assistant Professor and an Associate Professor with Tohoku University, from 2008 to 2017. He joined Denso Corporation, in 2018, where he is currently a Manager with the Materials Engineering Research and Development Division. His research interests include materials science, materials informatics, and machine learning.

TADASHI KADOWAKI received the B.Sc. degree from Tokyo Metropolitan University, in 1994, and the M.Sc. and Dr.Sc. degrees from the Tokyo Institute of Technology, in 1996 and 1999, respectively. He worked in academia and the semiconductor and pharmaceutical industries, from 1999 to 2018. He joined Denso Corporation, in 2018. His research interests include quantum physics, quantum computing, and optimization problems. He is a member of the Physical Society of Japan.